Construction of a destabilizing nonlinearity for discrete-time uncertain Lurye systems

Bálint Patartics*, Peter Seiler†, Joaquin Carrasco‡, and Bálint Vanek*

***Abstract*— This paper considers the instability of a Lurye system consisting of an uncertain, discrete-time, linear time-invariant plant in feedback with a slope-restricted nonlinearity. There is a large literature on analyzing the stability of such systems. This includes various conditions for proving stability of the Lurye system, including the Circle criterion and the use of O'Shea-Zames-Falb multipliers. In many cases, these conditions are sufficient but not necessary to prove stability. In contrast, there is also some work to construct specific nonlinearities that demonstrate the instability of the Lurye system (with the nominal plant dynamics). This paper considers a more general case where the plant has dynamic uncertainty. The goal is to construct both an instance of the uncertain model and a corresponding nonlinearity that combined make the Lurye system unstable. A limit cycle oscillation is also computed to verify the instability. A simple example is provided to demonstrate the results.**

I. Introduction

There is a large literature on robust stability of systems with uncertainties and/or nonlinear perturbations. This includes the structured singular value (also known as μ) analysis for uncertain Linear Time-Invariant (LTI) systems with dynamic and parametric uncertainty [1], [2], [3]. Computational methods have been developed to compute multipliers (also known as D/G-scales) that prove lower bounds on the robust stability margin [1], [2], [3], [4]. Moreover, there are methods to calculate an upper bound along with a corresponding instance of a destabilizing uncertainty. The most notable solution is the μ power iteration [5].

The Integral Quadratic Constraint (IQC) framework provides more general tools to assess the robust stability of uncertain systems with static or dynamic nonlinear elements in addition to LTI uncertainties [6]. Algorithms have been developed to compute multipliers that prove lower bounds on the robust stability margin. However, there are fewer results to compute upper bounds even though that calculation is often constructive and yields an instances of the destabilizing perturbation. The significance of the methods mentioned thus far is that they consider multiple sources of uncertainty at the same time. It is well known in the robust control literature that specific combinations of uncertainties often lead to stability issues that a loop-at-a-time analysis does not necessarily reveal [3, Section 9.6] [7].

Note that these frameworks, especially the IQC framework, have their roots in the absolute stability problem, which is concerned with the stability of the so-called Lurye system. In this paper, we consider the Lurye system as the feedback interconnection between a discrete-time, Single-Input Single-Output (SISO), LTI system and a slope-restricted, memoryless nonlinearity. The goal is to find a nonlinearity with minimal slope that, when combined with the plant, leads to a limit cycle oscillation of the Lurye system. Lower bounds on this minimal slope can be obtained using the circle criterion or the O'Shea-Zames-Falb multipliers [8], [9], [10], [11], [12], [13], [14].

However, the computation of an upper bound is a more challenging problem that has attracted less attention. The smallest destabilizing linear gain, called the Nyquist gain, provides a simple upper bound [15]. Recently, a method for calculating a tighter upper bound for Lurye systems was given in [16]. In contrast to the ad-hoc construction in [17] and [18], this method provides a systematic construction of the destabilizing nonlinearity corresponding to the upper bound.

In the present paper, we demonstrate that the automatic construction of a destabilizing nonlinearity in [16] can be extended to uncertain systems. This extension is critical for practical applications where the model is only an approximation of the real plant. This analysis is also relevant, since adverse combinations of the nonlinearity and uncertainty can cause unexpected stability issues that are not necessarily discovered when they are investigated separately, similarly to loop-at-a-time analysis.

The uncertainty is assumed as a single SISO dynamic block. Our goal is to obtain a nonlinearity with minimal slope and the corresponding uncertainty sample that destabilize the Lurye system. Similarly to [16], this calculation provides an upper bound on the stability margin but with uncertainty in the system also taken into account. This is achieved by presenting a graphical interpretation of the main result in [16] which is instrumental in obtaining a closed form solution.

The most closely related work is [19], that also considers the simultaneous presence of a nonlinearity and uncertainty. It builds on the describing function approach [20] which uses the linearization of the nonlinear component subjected to sinusoidal input. Hence, describing functions produce an approximation where only the first harmonic of the true input signal to the nonlinearity is considered. In [19], describing functions are applied to find an approximation of

[1]B. Patartics and B. Vanek are with the Institute for Computer Science and Control, Kende u. 13-17, H-1111 Budapest, Hungary (emails: patartics.balint@sztaki.hu and vanek@sztaki.hu)

[2]P. Seiler is with the Electrical Engineering & Computer Science Department, University of Michigan, 301 Beal Avenue Ann Arbor, MI 48109-2122, USA (email: pseiler@umich.edu)

[3]J. Carrasco is with the Department of Electrical & Electronic Engineering, University of Manchester, Oxford Rd. M13 9PL, Manchester, UK (email: joaquin.carrasco@manchester.ac.uk)

The research leading to these results is part of the FLiPASED project. This project has received funding from the Horizon 2020 research and innovation programme of the European Union under grant agreement No 815058.

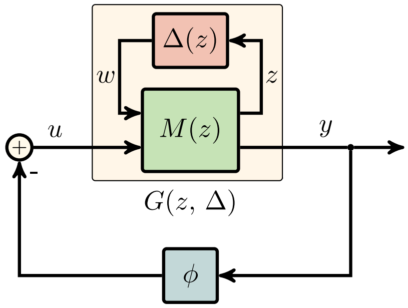

Fig. 1. Lurye system with uncertainty.

the destabilizing nonlinearity when the system is uncertain. No approximation is involved in the method presented in this paper, as the exact destabilizing nonlinearity is obtained.

The rest of the paper is structured as follows. The discrete-time uncertain Lurye stability problem is formulated in Section II. The preliminary results for nominal systems from [16] are given in Section III. Section IV contains the main contribution of the paper, i.e. the extension of the analysis method to uncertain systems with a SISO dynamic block. A numerical example is provided in Section V, and concluding remarks are made in Section VI.

II. Problem Formulation

Consider the Lurye system in Fig. 1 with a discrete-time, uncertain system $G(z,\,\Delta)$ in negative feedback with a nonlinearity $\phi : \mathbb{R} \longrightarrow \mathbb{R}$. The uncertain system $G(z,\,\Delta)$ is defined with the standard Linear Fractional Transformation (LFT) used in robust control [3]. Let $\mathbb{RH}_\infty$ denote the set of stable, rational, dicrete-time, LTI systems. Define the H_∞ norm of a stable LTI system Δ as the maximum gain of the system over all frequencies, i.e.

$$||\Delta||_\infty := \max_{\omega \in [0,\,\pi]} \bar{\sigma}\big(\Delta\big(e^{j\omega}\big)\big) \tag{1}$$

if $\Delta \in \mathbb{RH}_\infty$ and $||\Delta||_\infty = \infty$ otherwise. Here, $\bar{\sigma}\big(\Delta\big(e^{j\omega}\big)\big)$ denotes the largest singlular value of $\Delta\big(e^{j\omega}\big)$. Then $G(z,\,\Delta)$ is given by the interconnection of a 2×2 system $M \in \mathbb{RH}_\infty$ and a SISO uncertainty $\Delta \in \mathbb{RH}_\infty$ with $||\Delta||_\infty \leq 1$ as depicted in Fig. 1.

The transfer function $M(z)$ is partitioned as

$$M(z) = \begin{bmatrix} M_{11}(z) & M_{12}(z) \\ M_{21}(z) & M_{22}(z) \end{bmatrix}. \tag{2}$$

It is assumed that $G(z,\,\Delta)$ is robustly stable, i.e. it is stable for all $||\Delta||_\infty \leq 1$. By the small gain theorem [3, Theorem 9.1], this is equivalent to $||M_{11}||_\infty < 1$. The exact relation between $G(z,\,\Delta)$ and the entries of $M(z)$ is:

$$G(z,\,\Delta) = M_{22}(z) + \frac{M_{21}(z)\,M_{12}(z)\,\Delta(z)}{1 - M_{11}(z)\,\Delta(z)}. \tag{3}$$

Finally, the nonlinearity ϕ is assumed to have a slope between 0 and $k \geq 0$, i.e.

$$0 \leq \frac{\phi(y_2) - \phi(y_1)}{y_2 - y_1} \leq k \quad \forall y_1 \neq y_2. \tag{4}$$

$S(0,k)$ denotes the set of such slope-restricted nonlinearities. The special case $S(0,\infty)$ corresponds to monotone nonlinearities with no upper bound on the slope. We remark that the set $S(0,\infty)$ also includes multi-valued functions [16].

Our goal is to find the smallest $k^* \geq 0$ for which there exist an uncertainty $||\Delta^*||_\infty \leq 1$ and nonlinearity $\phi^* \in S(0,k^*)$ such that the Lurye system is unstable. This problem is challenging. Instead of a direct solution, lower bounds on k^* can be computed using IQCs [6] and O'Shea-Zames-Falb multipliers [9], [21]. This paper focuses on a complementary approach to obtain an upper bound on k^*. Specifically, we compute a $k_\mathrm{u} \geq k^*$ along with $\Delta_\mathrm{u}(z)$ and ϕ_u such that: (*a*) $||\Delta_\mathrm{u}||_\infty \leq 1$, (*b*) $\phi_\mathrm{u} \in S(0,\,k_\mathrm{u})$, and (*c*) the Lurye system of $G(z,\,\Delta_\mathrm{u})$ and ϕ_u has a limit-cycle oscillation.

III. Background: Results for Nominal Systems

This section briefly reviews existing methods for Lurye systems with no uncertainty [16]. These results form the basis for our main contribution with uncertainty in Section IV. To simplify notation, denote the nominal plant with $\Delta = 0$ by $G_0(z) := G(z,\,0)$. Let $\arg G_0\big(e^{j\omega}\big)$ be the phase of $G_0(z)$ at the frequency ω, i.e. the angle of $G_0\big(e^{j\omega}\big)$. In this paper, the phase is always understood to be between 0 and 2π. The following is the basic result for the nominal case.

Theorem 1 ([16]): Let $G_0 \in \mathbb{RH}_\infty$ and integers $0 < \alpha < \beta$ be given. Assume α and β are co-prime. Define the frequency $\omega := \frac{\alpha}{\beta}\pi$ with corresponding period $T = 2\beta$ if α is odd and $T = \beta$ if α is even. There exists a nonlinearity $\phi \in S(0,\,\infty)$ such that the Lurye system of G_0 and ϕ has a non-trivial T-periodic solution if

$$\pi - \frac{\pi}{T} \leq \arg G_0\big(e^{j\omega}\big) \leq \pi + \frac{\pi}{T}.$$

■

The full proof of Theorem 1 can be found in [16]. That proof relies on the following method for the construction of the exact nonlinearity ϕ that, when combined with the plant, leads to a limit cycle oscillation. Define $V_T := \big[1 \quad e^{j\omega} \ldots e^{j(T-1)\omega}\big]^T$, $U_T := \mathrm{Re}\, V_T$, and $Y_T := \mathrm{Re}\big(G_0\big(e^{j\omega}\big)\, V_T\big)$. If α is odd then construct a nonlinearity $\phi : \mathbb{R} \to \mathbb{R}$ by linearly interpolating Y_T and $-U_T$ within the range of Y_T, and extrapolating the first and last element of $-U_T$ outside the range of Y_T. The resulting nonlinearity is odd, it satisfies $\phi \in S(0,\,\infty)$, and it causes the Lurye system of G_0 and ϕ to have a T-periodic solution. The vectors U_T and Y_T are the limit cycle input/output signals of G_0 starting from the appropriate initial condition. If α is even then a similar construction can be made from U_T and Y_T as defined above. However, one additional step is required to compute a constant offset to U_T and Y_T so that $\phi(0) = 0$. Moreover, if α is even then the constructed nonlinearity is not necessarily odd.

Theorem 1 provides an analysis condition and nonlinearity construction at the fixed frequency $\omega = \frac{\alpha}{\beta}\pi$. Similarly to comparable robust stability tests [1], [2], this result is applied by choosing a sufficiently dense frequency grid and performing the computations at each point in the grid. This

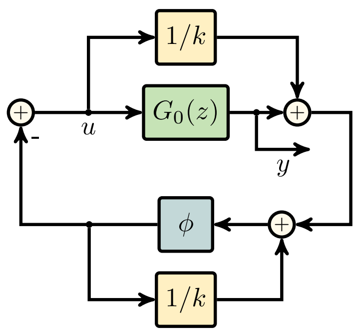

Fig. 2. Loop transformation that maps $S(0, k)$ to $S(0, \infty)$.

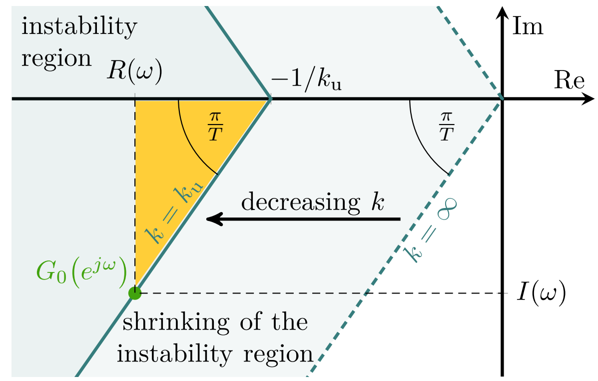

Fig. 3. Geometric interpretation of Theorem 2 and Corollary 1 with the response of the nominal system G_0 at a fixed frequency $\omega = \frac{\alpha}{\beta}\pi$.

amounts to choosing pairs of α and β that adhere to the assumptions of Theorem 1 ($0 < \alpha < \beta$, α and β are coprime) that in turn select a subset of $[0, \pi]$. Since the calculations involved in Theorem 1 are practically instantaneous, this is easily doable for a the range of $1 \leq \alpha, \beta \leq 100$ for example, which results in 3043 frequency points in $[0, \pi]$. In our experience, the computations over such a grid take no more than 3 seconds on a regular computer.

Theorem 1 is extended to slope-restricted nonlinearities in $S(0, k)$ with $k < \infty$ by the following result.

Theorem 2 ([16]): Let $G_0(z) \in \mathbb{RH}_\infty$ and integers $0 < \alpha < \beta$ be given. Assume α and β are co-prime. Define the frequency $\omega := \frac{\alpha}{\beta}\pi$ with corresponding period $T = 2\beta$ if α is odd and $T = \beta$ if α is even. There is $\phi \in S(0, k)$ with $k < \infty$ such that the Lurye system has a non-trivial T-periodic solution if

$$\pi - \frac{\pi}{T} \leq \arg\left[G_0\left(e^{j\omega}\right) + \frac{1}{k}\right] \leq \pi + \frac{\pi}{T}. \tag{5}$$

■

For the proof of this theorem, the reader is again referred to [16]. The main idea of the proof, which is also applied in this paper, is the application of the loop transformation in Fig. 2. Here, $\phi \in S(0, k)$, and the nonlinearity transformed by the feedback with the $1/k$ term belongs to $S(0, \infty)$ (hence possibly multi-valued).

Figure 3 provides a geometric interpretation of the condition in Theorems 1 and 2. The frequency response of G_0 at $\omega = \frac{\alpha}{\beta}\pi$ is depicted in the complex plane by the green dot. The blue dashed line in the figure marks the boundary of the guaranteed instability region. If $G_0\left(e^{j\omega}\right)$ is to the left of this boundary (as shown) then the Lurye system is unstable for some $\phi \in S(0, \infty)$. According to Theorem 2, the stability boundary shifts leftward when considering nonlinearities in $S(0, k)$ with decreasing values of k. The solid blue line in Fig. 3 corresponds to the limiting boundary. In other words, it gives a value k_u for which there is a nonlinearity in $S(0, k_u)$ causing the Lurye system to limit cycle with frequency ω. This minimum value, denoted k_u, is determined in the following corollary [22].

Corollary 1 ([22]): Let $G_0(z) \in \mathbb{RH}_\infty$ and integers $0 < \alpha < \beta$ be given. Assume α and β are co-prime. Define the frequency $\omega := \frac{\alpha}{\beta}\pi$ with corresponding period $T = 2\beta$ if α is odd and $T = \beta$ if α is even. Assume (5) in Theorem 2 holds. Let $G\left(e^{j\omega}\right) =: R(\omega) + jI(\omega)$ with the assumption that $R(\omega) < 0$. The smallest k, for which there is a nonlinearity in $S(0, k)$ that, when combined with the plant, leads to a limit cycle oscillation, is given by

$$k_u = \frac{-\sin\left(\frac{\pi}{T}\right)}{|I(\omega)|\cos\left(\frac{\pi}{T}\right) + R(\omega)\sin\left(\frac{\pi}{T}\right)}. \tag{6}$$

Proof: Based on the highlighted triangle in Fig. 3, k_u has to satisfy the equation

$$\tan\left(\frac{\pi}{T}\right) = \frac{I(\omega)}{R(\omega) + \frac{1}{k_u}}. \tag{7}$$

This equation is true if $I(\omega) \leq 0$. Solve for k_u to obtain

$$k_u = \frac{\tan\left(\frac{\pi}{T}\right)}{I(\omega) - R(\omega)\tan\left(\frac{\pi}{T}\right)}. \tag{8}$$

Rewrite $\tan\left(\frac{\pi}{T}\right)$ in terms of $\sin\left(\frac{\pi}{T}\right)$ and $\cos\left(\frac{\pi}{T}\right)$ and use the symmetry of the problem to replace I with $|I|$. This yields (6). ■

It is emphasized that k_u given in Corollary 1 is only an upper bound on the true stability boundary. Specifically, let $k^* \geq 0$ denote the smallest value for which there exists a nonlinearity $\phi^* \in S(0, k^*)$ such that the Lurye system of the nominal plant G_0 and ϕ^* is unstable. Theorem 2 gives a condition that is sufficient (but not necessary) for the existence of a destabilizing nonlinearity. Hence the value of k_u given in Corollary 1 is only an upper bound, i.e. $k_u \geq k^*$.

IV. Results for Uncertain Systems

The main result of the paper is presented in this section. First, it is shown that for a fixed frequency ω, the image of the function $G\left(e^{j\omega}, \delta\right)$ for $\delta \in \mathbb{C}$, $|\delta| \leq 1$ is a disk in the complex plane. Then, a geometric argument, similar to that in the proof of Corollary 1, is used to derive k_u for the destabilizing nonlinearity with the uncertain plant.

The next lemma states that $G\left(e^{j\omega}, \delta\right)$ in (3) maps the unit circle $|\delta| = 1$ to a circle. With some abuse of notation, we drop the dependence on frequency and treat the entries of M

as complex variables in the lemma. Moreover, the complex conjugate of $z \in \mathbb{C}$ is denoted by $\overline{z}$.

Lemma 1: Consider the function $G : \mathbb{C} \longrightarrow \mathbb{C}$ defined by:

$$G(\delta) := M_{22} + \frac{M_{21} M_{12} \delta}{1 - M_{11}\delta} \tag{9}$$

with $M_{11},\, M_{12},\, M_{21},\, M_{22} \in \mathbb{C}$, and $|M_{11}| < 1$. G maps the unit circle $\{e^{j\vartheta} : \vartheta \in [0,\, 2\pi]\}$ to the circle $\{C + \varrho e^{j\vartheta} : \vartheta \in [0,\, 2\pi]\}$ with center and radius defined by:

$$C := M_{22} + \frac{\overline{M}_{11} M_{21} M_{12}}{1 - |M_{11}|^2} \quad \text{and} \quad \varrho := \frac{|M_{21} M_{12}|}{1 - |M_{11}|^2}. \tag{10}$$

Proof: The statement of the lemma follows from standard complex analysis results [23]. ■

Hence, it is established that for fixed ω, $\{G\big(e^{j\omega},\, e^{j\vartheta}\big) : \vartheta \in [0,\, 2\pi]\}$ is a circle. It can also be shown that the interior of the unit circle is mapped to the interior of the circle given by the center and radius in (10). Thus the image of $G\big(e^{j\omega},\, \Delta\big)$ for $||\Delta||_\infty \le 1$ is indeed a disk in the complex plane at each frequency.

For simplicity, the remainder of the section omits the dependence of the variables on the frequency, e.g. the entries of M are written without the $e^{j\omega}$ argument. The unit disk is mapped by $G\big(e^{j\omega},\, \Delta\big)$ to a disk with center C and radius ϱ as defined in (10). We differentiate between two distinct cases when calculating the worst-case uncertainty and nonlinearity: (*a*) the disk with center C and radius ϱ touches the side of the instability boundary as in Fig. 4 (Section IV-A) and, (*b*) the disk touches the corner of the instability boundary (Section IV-B).

A. Disk touches the side of the instability boundary

Let C_R and C_I denote the real and imaginary parts of C. The frequency response of the uncertain system at a fixed frequency is illustrated in Fig. 4 for the case when $C_I < 0$. Using the symmetry of problem, it is easy to write the following results so that they are true for any sign of C_I, i.e. in terms of $|C_I|$. In this section, it is assumed that $|C_I| > \varrho \cos\big(\frac{\pi}{T}\big)$, which means that the uncertainty disc is "sufficiently" far from the real axis. Section IV-B describes the case when this assumption is violated.

Taking the symmetry of the problem into account, the highlighted triangle in Fig. 4 reveals that

$$\tan\Big(\frac{\pi}{T}\Big) = \frac{|C_I| - \varrho\cos\big(\frac{\pi}{T}\big)}{-\frac{1}{k_\mathrm{u}} - C_R + \varrho \sin\big(\frac{\pi}{T}\big)}. \tag{11}$$

Note that this is only true if $|C_I| > \varrho\cos\big(\frac{\pi}{T}\big)$ since otherwise the worst-case point is on the real axis. Solve for k_u to obtain

$$k_\mathrm{u} = \frac{\sin\big(\frac{\pi}{T}\big)}{\varrho - C_R \sin\big(\frac{\pi}{T}\big) - |C_I|\cos\big(\frac{\pi}{T}\big)}. \tag{12}$$

Denote the point where the circle touches the instability boundary by $G_\mathrm{u} = C + \varrho e^{j\vartheta_\mathrm{u}}$. Based on Fig. 4,

$$\vartheta_\mathrm{u} = -\mathrm{sign}(C_I)\left(\frac{\pi}{2} + \frac{\pi}{T}\right). \tag{13}$$

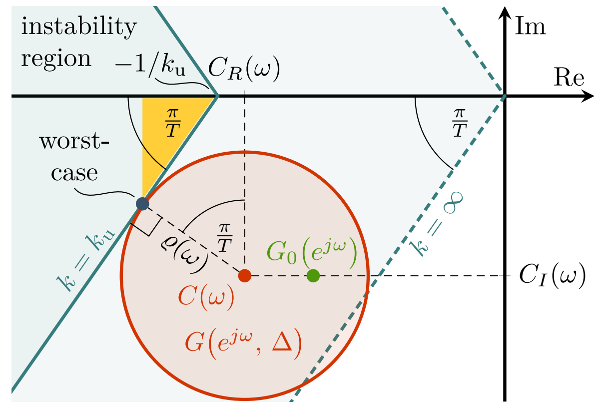

Fig. 4. Geometric interpretation of the main result with the response of the uncertain system $G(z,\, \Delta)$ at a fixed frequency $\omega = \frac{\alpha}{\beta}\pi$.

To express the worst-case uncertainty, write G_u as

$$G_\mathrm{u} = M_{22} + \frac{M_{21} M_{12} \delta_\mathrm{u}}{1 - M_{11}\delta_\mathrm{u}}, \tag{14}$$

where $\delta_\mathrm{u} \in \mathbb{C}$, $|\delta_\mathrm{u}| = 1$ is the value of the uncertainty at the frequency ω. Expressing δ_u, we get

$$\delta_\mathrm{u} = \frac{G_\mathrm{u} - M_{22}}{M_{21}M_{12} + (G_\mathrm{u} - M_{22})\, M_{11}}. \tag{15}$$

The LTI worst-case uncertainty $\Delta_\mathrm{u}(z)$ is obtained by interpolating δ_u by a stable all-pass system. Lemma 2 in Appendix A proves that this is always possible and provides the interpolation method that results in $\Delta_\mathrm{u}(z)$. We remark that δ_u can also be interpolated with a nonrational LTI system and the resulting interpolant yields the same limit cycle.

B. Disk touches the corner of the instability boundary

As explained in Section IV-A, the derivation there is not valid if $|C_I| \le \varrho\cos\big(\frac{\pi}{T}\big)$. In this case, the worst-case corresponds to the uncertainty disk touching the point where the stability boundary intersects the real axis. Hence, the distance between C and the $-1/k_\mathrm{u}$ point is ϱ, i.e.

$$\left(C_R + \frac{1}{k_\mathrm{u}}\right)^2 + C_I^2 = \varrho^2. \tag{16}$$

From this,

$$k_\mathrm{u} = \frac{1}{\sqrt{\varrho^2 - C_I^2} - C_R}. \tag{17}$$

The worst-case point on the disk is $G_\mathrm{u} = -1/k_\mathrm{u}$. Substituting this into (15) yields

$$\delta_\mathrm{u} = \frac{-\frac{1}{k_\mathrm{u}} - M_{22}}{M_{21}M_{12} - \Big(M_{22} + \frac{1}{k_\mathrm{u}}\Big)\, M_{11}}. \tag{18}$$

The worst-case LTI uncertainty $\Delta(z)$, that interpolates δ_u at frequency ω, is again obtained by applying Lemma 2 in Appendix A.

We remark that in this case, the destabilizing nonlinearity is a linear gain, i.e. $\phi_\mathrm{u} = k_\mathrm{u}$. We established in the derivation above that $G\big(e^{j\omega},\, \Delta_\mathrm{u}\big) = G_\mathrm{u} = -1/k_\mathrm{u}$. Hence,

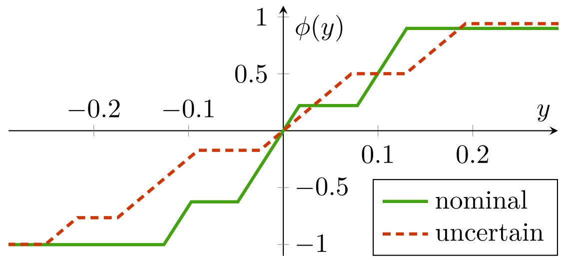

Fig. 5. Nonlinearities obtained for the numerical example.

$k_{\mathrm{u}} G\big(e^{j\omega}, \Delta_{\mathrm{u}}\big) + 1 = 0$. Then, the Nyquist criterion implies that the Lurye system with $G(z, \Delta_{\mathrm{u}})$ and $\phi_{\mathrm{u}} = k_{\mathrm{u}}$ enters into a limit cycle with frequency ω.

C. Limit cycle in the time domain

The limit cycle with the input and output series U_T and Y_T is not necessarily attractive. Hence, the system usually only exhibits the oscillation in the time domain with the right initial conditions. These initial conditions are derived next. Assume the state-space representation of $G(z, \Delta_{\mathrm{u}})$ is given. For any initial state x_0 and input series U, the output series of the system is $Y = \Phi x_0 + \Gamma U$, where Φ and Γ are composed of the state-space matrices. Construct Y and U by stacking Y_T and U_T enough times so that $\dim Y = \dim U = \dim x_0$, and calculate the initial condition as $x_0 = \Phi^{-1}(Y - \Gamma U)$.

V. Numerical Example

A numerical example is provided to illustrate the results of Section IV. The nominal system,

$$G_0(z) = \frac{0.1z}{z^2 - 1.8z + 0.81}, \tag{19}$$

is taken from Example 1 in [13]. This example also occurs in [17] and [18] where conditions for a limit cycle oscillation are constructed by hand. In contrast, the systematic construction of Section IV is demonstrated next with uncertainty added to the example. The uncertain system is obtained by introducing 15% uncertainty across all frequencies, i.e. $G(z, \Delta) = G_0(z)\,(1 + 0.15\Delta(z))$, where $||\Delta||_\infty \leq 1$. This system is written as $G(z, \Delta) = \mathcal{F}_U(M(z), \Delta(z))$ with

$$M(z) = \begin{bmatrix} 0 & 0.15 \\ G_0(z) & G_0(z) \end{bmatrix}. \tag{20}$$

First, consider the nominal system $G_0(z)$ in which case Theorem 2 and Corollary 1 is applied to construct a destabilizing nonlinearity. We conduct these calculations on the frequency grid $\{\frac{\alpha}{\beta}\pi : \alpha$ and β are relative primes, $1 \leq \alpha < \beta \leq 100\}$, which is found sufficiently dense, as increasing its density any further does not change the results. The critical frequency of $2\pi/7$ is obtained with the slope bound $k_{\mathrm{u},0} = 13.03$. The corresponding nonlinearity is constructed using the method in the proof of Theorem 1. The result is depicted by the solid green line in Fig. 5.

Next, consider the effect of the uncertainty using the results given in Section IV. Note that $||M_{11}||_\infty = 0 < 1$ so that the uncertain system $G(z, \Delta)$ is robustly stable. The resulting critical frequency is $2\pi/9$, and the slope bound shrinks to $k_{\mathrm{u}} = 6.96$ which is noticeably smaller than $k_{\mathrm{u},0} = 13.03$. The worst-case uncertainty sample at the critical frequency is $\delta_{\mathrm{u}} = 0.06 - 0.99j$. The interpolation technique in Appendix A yields $\Delta_{\mathrm{u}}(z) = \frac{1-0.44z}{z-0.44}$. The constructed destabilizing nonlinearity is depicted by the dashed red line in Fig. 5. The figure shows that the presence of the uncertainty makes this nonlinearity substantially different compared to the nominal case.

Fig. 6 is a graphical representation of the phase condition of Theorem 2 over a frequency grid. Note that in Theorem 2, only the frequency points that are rational fractions of π are considered. In Fig. 6, the dots corresponding to those frequencies are connected to make the data easier to interpret, but the connecting lines have no meaning (other than for visual purposes). The phase bounds $\pi \pm \frac{\pi}{T}$ in (5), which demarcate the boundary of the instability region, are represented by the light blue dots around π, in the bottom of the figure. The red area shows the range of values the phase can attain with the variation of the uncertainty. If we decrease k below k_{u}, this area moves away from the boundary of the instability region, while increasing k moves it further into the instability region. The enlarged section on the right demonstrates that for $k = k_{\mathrm{u}} = 6.96$, the uncertain area touches the boundary at the critical frequency $2\pi/9$. At all other frequency points on the grid, the uncertain area is outside the instability region.

Finally, a time domain simulation is presented. Fig. 7 depicts the output of the Lurye system in Fig. 1 for random samples of the uncertainty as well as for the nominal ($\Delta(z) = 0$) and worst-case ($\Delta(z) = \Delta_{\mathrm{u}}(z)$) values. For all samples, the initial conditions are chosen such that the input and output sequence of the systems most closely resemble the sequence corresponding to the limit cycle. The initial state is determined by finding the least-squares optimal solution of the equation $Y = \Phi x_0 + \Gamma U$ from Section IV-C. Fig. 7 demonstrates that the amplitude of the oscillation decays for the nominal system and for random samples of the uncertainty, but the system with Δ_{u} enters into a sustained limit cycle. This illustrates the combined effect of the uncertainty and nonlinearity can coupling together to create a limit cycle instability.

VI. Conclusions

A method is presented for the instability analysis of a discrete-time Lurye system in the presence of a SISO dynamic uncertainty block and a slope-restricted nonlinearity. An upper bound of the minimal slope is determined for which there exist a nonlinearity and a worst-case uncertainty that can cause the Lurye system to enter into a limit cycle oscillation. The destabilizing nonlinearity and uncertainty sample are also constructed. A numerical example is given that demonstrates how the presence of uncertainty decreases the required slope of the destabilizing nonlinearity compared to the nominal case.

References

[1] J. Doyle, "Analysis of feedback systems with structured uncertainties," in *IEE Proceedings D-Control Theory and Applications*, vol. 129, no. 6. IET, 1982, pp. 242–250.

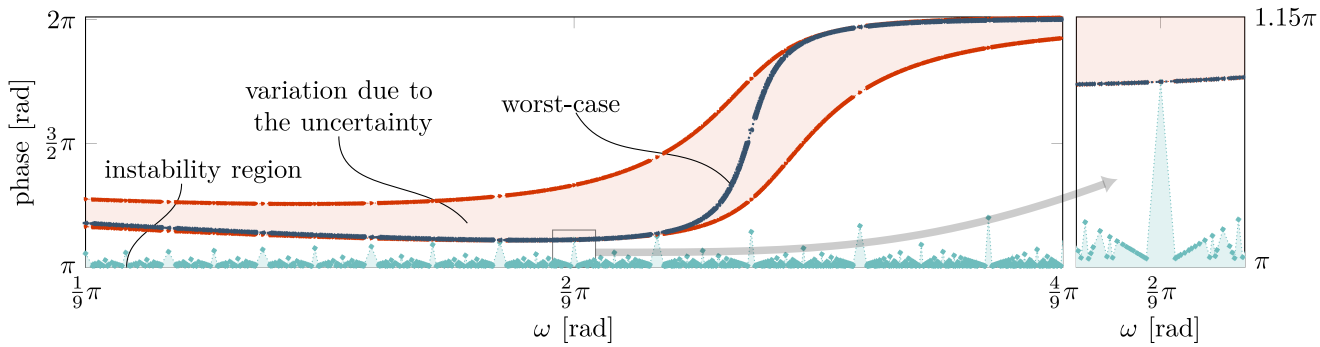

Fig. 6. Phase of the system $G(z, \Delta) + 1/k_{\mathrm{u}}$ in the example ($k_{\mathrm{u}} = 6.96$). The phase values are only valid for frequencies that are rational fractions of π (see Theorem 2). The lines connecting these points only serve as visual guides.

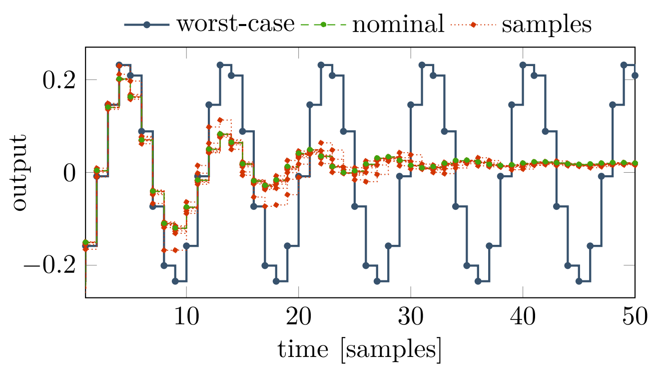

Fig. 7. Time domain simulation for the example with the nominal, worst-case and 20 random samples of the uncertainty.

[2] A. Packard and J. Doyle, "The complex structured singular value," *Automatica*, vol. 29, no. 1, pp. 71–109, 1993.

[3] K. Zhou, J. C. Doyle, and K. Glover, *Robust and optimal control*. Prentice hall New Jersey, 1996, vol. 40.

[4] P. M. Young, "Robustness with parametric and dynamic uncertainty," Ph.D. dissertation, California Institute of Technology, 1993.

[5] P. Young and J. Doyle, "A lower bound for the mixed-μ problem," *IEEE Transactions on Automatic Control*, vol. 42, no. 1, pp. 123–128, 1997.

[6] A. Megretski and A. Rantzer, "System analysis via integral quadratic constraints," *IEEE Trans. on Aut. Control*, vol. 42, no. 6, pp. 819–830, 1997.

[7] P. Seiler, A. Packard, and P. Gahinet, "An introduction to disk margins [lecture notes]," *IEEE Control Systems Magazine*, vol. 40, no. 5, pp. 78–95, 2020.

[8] R. O'Shea and M. Younis, "A frequency-time domain stability criterion for sampled-data systems," *IEEE Transactions on Automatic Control*, vol. 12, no. 6, pp. 719–724, December 1967.

[9] G. Zames and P. L. Falb, "Stability conditions for systems with monotone and slope-restricted nonlinearities," *SIAM J. Control*, vol. 6, pp. 89–108, 1968.

[10] J. C. Willems and R. Brockett, "Some new rearrangement inequalities having application in stability analysis," *IEEE Transactions on Automatic Control*, vol. 13, no. 5, pp. 539–549, October 1968.

[11] J. C. Willems, *The analysis of feedback systems*. MIT Press, 1971.

[12] M. Fetzer and C. W. Scherer, "Absolute stability analysis of discrete time feedback interconnections," *IFAC-PapersOnLine*, vol. 50, no. 1, pp. 8447–8453, 2017.

[13] J. Carrasco, W. P. Heath, J. Zhang, N. S. Ahmad, and S. Wang, "Convex searches for discrete-time Zames-Falb multipliers," *IEEE Transactions on Automatic Control*, vol. 65, no. 11, pp. 4538–4553, 2020.

[14] M. C. Turner and R. Drummond, "Discrete-time systems with slope restricted nonlinearities: Zames-Falb multiplier analysis using external positivity," *International Journal of Robust and Nonlinear Control*, vol. 31, no. 6, pp. 2255–2273, 2021.

[15] J. C. Willems, "Mechanisms for the stability and instability in feedback systems," *Proceedings of the IEEE*, vol. 64, no. 1, pp. 24–35, 1976.

[16] P. Seiler and J. Carrasco, "Construction of periodic counterexamples to the discrete-time Kalman conjecture," *IEEE Control Systems Letters*, vol. 5, no. 4, pp. 1291–1296, 2020.

[17] J. Carrasco, W. P. Heath, and M. de la Sen, "Second-order counterexample to the discrete-time Kalman conjecture," in *European Control Conference*, 2015, pp. 981–985.

[18] W. P. Heath, J. Carrasco, and M. de la Sen, "Second-order counterexamples to the discrete-time Kalman conjecture," *Automatica*, vol. 60, pp. 140–144, 2015.

[19] J. E. Tierno, "Describing function analysis in the presence of uncertainty," *Journal of Guidance, Control, and Dynamics*, vol. 20, no. 5, pp. 956–961, 1997.

[20] A. Gelb and W. E. Vander Velde, *Multiple-input describing functions and nonlinear system design*. McGraw-Hill, New York, 1968.

[21] J. Carrasco, M. C. Turner, and W. P. Heath, "Zames-Falb multipliers for absolute stability: From O'Shea's contribution to convex searches," *European Journal of Control*, vol. 28, pp. 1–19, 2016.

[22] J. Zhang, J. Carrasco, and W. P. Heath, "Duality bounds for discrete-time Zames-Falb multipliers," *IEEE Transactions on Automatic Control*, 2021.

[23] D. Zill and P. Shanahan, *A first course in complex analysis with applications*. Jones & Bartlett Learning, 2009.

Appendix

A. SISO interpolation

Lemma 2 below provides an discrete-time interpolation result. A similar result for continuous-time systems is given in the proof of Theorem 9.1 (Small Gain Theorem) of [3].

Lemma 2: Given are a frequency $\omega_0 \in [0, \pi]$, and a complex number $\delta_0 \in \mathbb{C}$ with $|\delta_0| = 1$. There exists a SISO LTI system $\Delta(z) \in \mathbb{RH}_\infty$ such that $\Delta(e^{j\omega_0}) = \delta_0$ and $||\Delta||_\infty \leq 1$.

Proof: Consider the system $F(z) = \frac{1-pz}{z-p}$. For any $p \in \mathbb{R}$ and $\omega \in [0, \pi]$, $|F(e^{j\omega})| = 1$. Write $\delta_0 = e^{j\vartheta_0}$ and choose $\Delta(z) = F(z)$ with

$$p = -\frac{\sin\frac{\omega_0+\vartheta_0}{2}}{\sin\frac{\omega_0-\vartheta_0}{2}}. \tag{21}$$

If $\sin(\omega_0)\sin(\vartheta_0) < 0$, then $|p| < 1$ and hence $\Delta(z) \in \mathbb{RH}_\infty$. Otherwise set $\Delta(z) = -F(z)$ with

$$p = \frac{\cos\frac{\omega_0+\vartheta_0}{2}}{\cos\frac{\omega_0-\vartheta_0}{2}} \tag{22}$$

to obtain the stable interpolant. ∎